Wind Farm Connected Distribution Line Fault Detection using Symmetrical Nature of Mean

Das Prakash Chennamsetty*‡ iD, Sravana Kumar Bali** iD

*,** Department of Electrical and Electronics Engineering, GITAM School of Technology, GITAM Deemed to be University, Visakhapatnam, India-530045

(dasprakash.ch@gmail.com *, sravanbali@gmail.com **)

‡ Corresponding Author; Das Prakash Chennamsetty, GITAM Deemed to be University, dasprakash.ch@gmail.com

Abstract- A new statistical fault detection method is proposed in this paper to detect the faults in the distribution lines connected with wind farms. The approach is designed with the help of symmetrical nature of current signals during normal conditions of the system to detect the faults using the non-linearity segment. For this purpose, statistical mean of $1/4^{th}$ cycle of current information is used with shifting window mechanism. The method utilize direct instantaneous signal information reduces the computational burden and increases the speed of the decision. The method is tested on wide class of unsymmetrical and symmetrical faults with different fault parameters. The influence of the location, inception angle and resistance of the faults are simulated to test the efficacy of the proposed method. Further, the investigations of the proposed methods are extended to variable wind system conditions to check the adaptability of the method. All the simulations are carried out on a 25 kV, 9 MW wind farm connected to grid using MATLAB-SIMULINK.

Keywords Wind farm, Statistical mean, Fault detection, symmetrical faults.

1. Introduction

The symmetrical nature of the signal variations are helpful to detect the faults in normal transmission lines. Conventional techniques based on sample and cycle information useful to detect such signal distortions. Recently, integration of wind and solar increases the operational challenges especially from protection side. Therefore, fault detection is a challenging task in such systems. The wind and solar generation is integrated to grid through distribution lines and protection challenges need to be addressed in these areas [1]-[2]. A detailed review is provided to show the overview of the earlier research studies.

The fault diagnosis of the wind integrating distribution system and transmission lines classified into three tasks namely, fault detection, faulty phase identification and fault classification, fault location [3]. After initiation of the fault, the instantaneous current magnitude increases, and it is detected by the fault detector (FD). Once fault detection task in completed, the faulty component is isolated from the rest of the system. Fault classification and location are the post fault diagnosis works [4]. Therefore, careful design of FD is important for more secure and reliable system. Conventional

distance relays and differential relays are suitable for normal power transmission networks and are extended to renewable penetrated networks [5]-[9].In case of wind penetrated networks, the fluctuations in grid side voltage, current and power due to continuous variation of wind speed trigger the adaptiveness of the distance relay. In [5], the boundaries of the distance relay are set by considering the variations of the wind and system parameters. The adaptivity of trip characteristics are achieved with artificial neural networks(ANN) in [6]. In detail, local information of wind units are associated with ANN to develop the characteristics of the zone settings to avoid mal operation of the distance relays. Furthermore, the distance relay measured impedance used to locate the faults in conventional systems. However, it doesn't reflect the accurate location in wind farm fed induction generator-based systems due to dynamic variations of the system. In particular, the impedance failed to represent the fault location a few cycles after occurrence of symmetrical fault. The counter measures of such problems are presented in [7]. Several works are reported in the consequent years and recently a new method is presented in [8] using the geometric distribution characteristics (GDC) of the lines connected to wind farms called collector lines. Using the GDC of the

collector line information of voltage and current, an adaptive distance protection strategy is used to classify the faulty line along with the fault detection. Differential relays are also useful to detect, classify and locate the faults in transmission networks integrating with high penetration of renewables. The combined approaches are available in literature to produce reliable outputs during faults [9]. In [9], a method is provided based on the combination of distance and differential protection. Since the calculated impedance is the effected factor in wind integrating systems, the method utilizing the information of active power at both ends to estimate the fault resistance. The method handled typical cases better than existing distance and differential relay schemes. Apart from the distance and differential schemes, few other approaches are available in existing research findings. In [10], current phase comparison pilot scheme is provided to protect the distributed lines with distribution generation. Instead of the single end information, both end information improve the protection attributes and enhance the security and reliability of the schemes. In line, an impedance angle-based differential algorithm is proposed in [11] to protect the microgrid. The scheme is implemented with two terminal information provided reliable decisions during typical faults. The change in the information of the voltage and current is identified by enhancing the features of the information. This task is fulfilled by signal processing tools such as wavelet transform (WT), S-transform and Hilbert transform etc. With availability of the large input features, artificial intelligent techniques are helpful to adopt correct and reduced information of extended input features. Such type of the works are available in [12]-[15]. In [12], WT is used to detect the faults in DG penetrated network. In case of DG, islanding event need to be discriminated from faults to improve the protection attributes of the algorithm. In [13], support vector machine is used to classify the grid faults conditions and islanding events. In [14], extreme learning machine is used to protect the microgrid in presence of intermittency of the wind speed. In [15], Hilbert-Huang transform is used to implement the differential scheme to protect microgrid consist of renewable DG's. Apart from these intelligent tools, few methods are available based on signal symmetry. In [16], both fault detection and faulty phase classification tasks are achieved with transient energy indices. In [17], positive sequence component based differential scheme is presented to protect wind integrated network with additional support from meta heuristic algorithm. Most of these works are related to wind integrated networks and few works are available on photovoltaic penetration [18]-[20]. All these works reported from [4]-[20] utilizing complex mechanisms to protect the renewable penetrated networks [21]-[26].

In this paper, signal symmetrical nature mean-based technique is proposed to detect the faults in the distributed lines connected to wind farms. The method is also extended to identify the faulty phases after detection. To implement this method, 3-phase currents are measured at grid connecting point and processed through proposed SNM method. The efficacy of the method is proved with extensive simulations by varying the types of faults, location of faults, inception times of fault and fault resistances. Furthermore, a separate comparison are provided to show the merits of the method

over other popular methods in terms of speed and dependability. The method is simple, easy to implement, provide quick decision during faults and robust. The details of the proposed method are provided in section 2. Test system details are provided in section 3. Simulation results are presented in section 4 and comparisons in section 5. Finally, conclusions are listed in section 6.

2. Proposed Method

During the normal operating conditions, the instantaneous phase current of the test system mathematically expressed with a sinusoidal function and provided in the discrete form to implement proposed fault detector in the digital relays shown in Equation (1)

$$i_p(n) = I_P \sin\left(2\pi f_o \left(\frac{n}{f_s}\right) + \varphi\right), n = 0,1,2,\dots N \quad (1)$$

In Equation (1), p is the phase, f_o is the fundamental frequency, φ is the phase angle shift w.r.to reference frame in radians/sec, f_s is the sampling frequency. Since the method is framed based on the number of the samples of the $1/4^{th}$ cycle of the signal, it is necessary to express the Equation (1) based on the number of samples of the full cycle of the instantaneous current signal. The remodified expression of equation (1) is given by

$$i_p(n) = I_P \sin\left(2\pi \left(\frac{n}{N_f}\right) + \varphi\right) \quad (2)$$

In equation (2), N_f is the number of samples of one full cycle of the instantaneous current signal whose value is the ratio of sampling frequency and system operating frequency is shown in Equation (3)

$$N_f = \frac{f_s}{f_o} \quad (3)$$

For the $1/4^{th}$ sub cycle, the number of the samples are $\frac{N_f}{4}$ considered into a single window and all the samples mean is considered as fault detection metric. The number of samples in each window is same during the normal and fault situations as shown in Figure 1. However, the mean values of the samples inserted in the windows during the normal condition are same due to the symmetry nature of the current signal. With initiation of fault in the system, the current amplitude abruptly increases/decreases and therefore the mean metric differs from the pre-fault measure. This unique feature of the instantaneous current signal useful to detect faults in the system and discriminate them from normal condition to isolate the faulty components from the rest of the system.
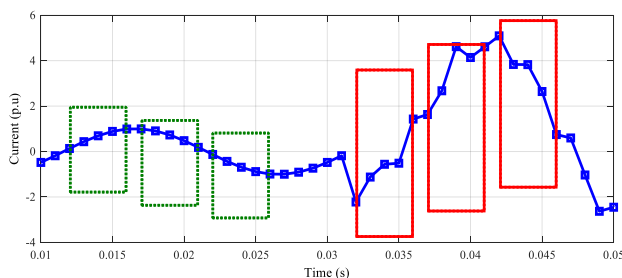
Fig.1. Shifting window mean calculation in current signal during normal and fault conditions.

Suppose the mean of the samples in the 1/4th cycle window is i_{Si_mean} and which is constant during the normal operating conditions of the system due to signal symmetry. The expression is given by

$$i_{Si\_mean} = \pm k_1 , i = 1,2,\dots P \qquad (4)$$

The value of the P is equal to 4 times of total cycles of the signal since one cycle is equal to 4 quarter cycles and therefore, P mean values are possible in each case. During the faults and the disturbances, this mean value exceeds from nominal value $\pm k_1$. To make the detection process comfortable, absolute value of the mean is considered in each window instead of actual value. To record faults, the decision logic is given by

$$i_{Si\_mean} \geq \theta \qquad (5)$$

The value of θ is called pre-defined threshold to detect the disturbances. However, it is important to discriminate the faults from other non-fault disturbances. To discriminate faults, a proper threshold is required and the feasible value of the threshold to detect all types of faults is given by

$$\theta > k_1 \qquad (6)$$

The pre-defined threshold is k_1 identified by using the normal condition signal monitoring. During normal conditions, the absolute mean of all the samples in each sliding window is same. For example, the values in between 0° to 90^0 are 0, 18, 36, 54, 72 and 90 and 90° to 180° are 90, 108, 126, 144, 162 and 180 possess same trigonometric values and the calculated mean is also same from these samples. However, the value changes with disturbance condition detected using the equation (6).

3. Test System

To test the performance of the proposed SNM-based fault detection and faulty phase identification method, 9 MW of wind farm connected to 25 KV distribution system exports electrical power to grid operated at 120 KV. The length of the distribution line is 30 km. The wind turbines Doubly fed induction generator (DFIG) used by wind turbines consist of a wound rotor induction generator and an AC-DC-AC based

pulse width modulation (PWM) converter with IGBT's with a total number of 6 units each of 1.5 MW capacity. The test system operated at 60 Hz is modelled in SIMULINK and signals are sampled at 1 kHz and algorithm is tested using MATLAB R2018a software. Three phase π network is used in the simulations of the distribution line to create the faults with the positive and zero sequence resistances of 0.0201Ω/km and 0.1065 Ω/km respectively. The positive, zero sequence inductances are 0.7611 mH/km, 2.301 mH/km, capacitances are 11.33 µF/km and 5.01 µF/km respectively.
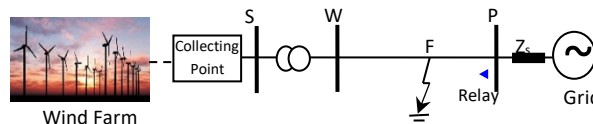

Fig. 2. Single line diagram of the test system [22]

4. Simulation Results

The signal symmetrical nature deviates from the regular sinusoidal structure due to inception of fault and/or other disturbances. The deviation in faults comparatively larger in magnitude compared to other disturbances such as noise in signal, harmonics, spikes, capacitor switching and load disturbances. This unique feature of the proposed algorithm is useful to detect all types of the faults involving single-phase-to-ground, line-to-line, line-to-line-ground, and three phase faults. Wide range of simulations are carried out to test the efficacy of the proposed method to validate the performance of the proposed scheme.

4.1. Line-to-ground faults

The line-to-ground faults occurs 85% times of overall fault incidents. The detection magnitude of the line-to-ground faults is comparatively small due to single phase involvement in the fault. Both criterions of occurrence of faults and index magnitude are considered in this paper to validate the performance of the proposed approach. For this purpose, three different single line-to-ground faults are considered to carry simulation studies. An A-g fault is created at 12 km from the grid-side initiated at inception time of 1.4 sec with a fault resistance of 8Ω and corresponding current signals are retrieved at relay point. This current information is further processed through the proposed detection scheme to identify the occurrence of faults. Both current and detection indices are plotted in Figure 3 for the A-g fault. Similar to A-g fault, B-g and C-g faults are simulated at different fault operating conditions to check the performance of the proposed scheme. In case of B-g fault, fault location of 22 km, fault inception time of 1.5 sec and fault resistance of 5Ω are considered to investigate the performance of the method. In case of C-g fault, fault location of 10 km, fault inception time of 1.6 sec and fault resistance of 20Ω are considered to investigate the performance of the method. The responses of the proposed method during B-g and C-g faults are shown in Figures 4 and 5 respectively.
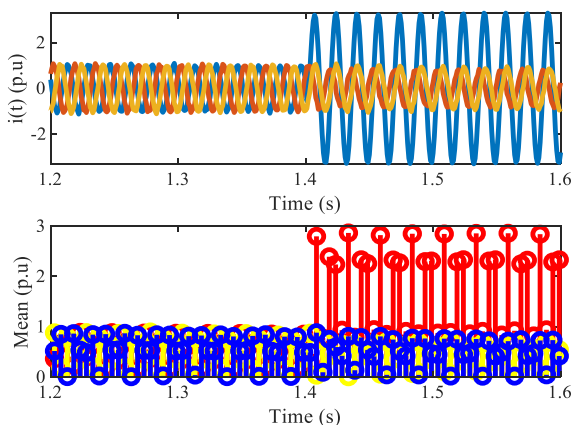
Fig. 3. SNM-based method output during A-g Fault, a. currents, b. Means.
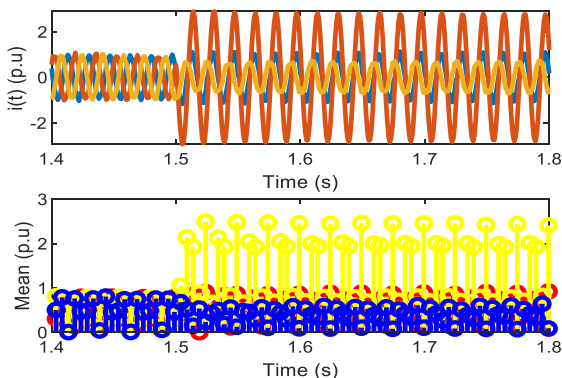
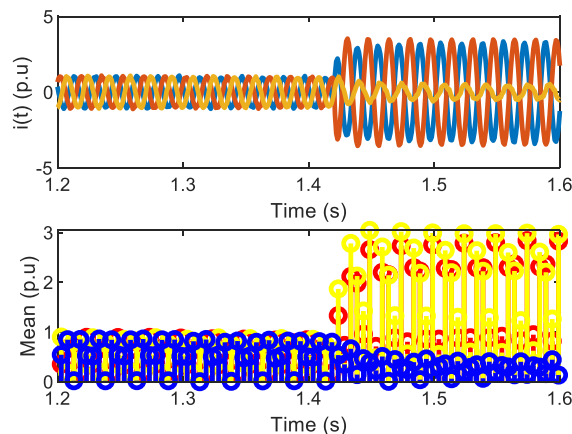**Fig. 4.** SNM-based method output during B-g Fault, a. currents, b. Means
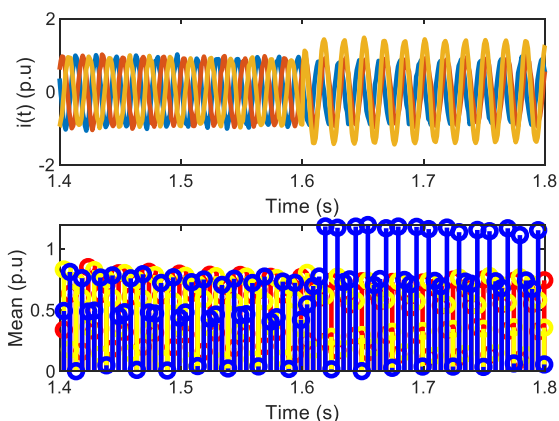
Fig. 5. SNM-based method output during C-g Fault, a. currents, b. Means

The mean values of each phase during the normal condition is same as discussed in section 4 equal to 1 as shown in Figures 3, 4 and 5 before fault inceptions 1.4, 1.5 and 1.6 sec. With initiation of the fault, the mean values are increased from their nominal values based on the type of fault. In case of A-g fault, the index corresponding to A-phase rises from 1 due to fault. However, other indices corresponding to B and C phases are remained unaltered since they are non-faulty phases. This feature useful to classify the faulty phase along

with the fault detection. Similar observations are extracted in the Figure 4 and Figure 5 with respect to B-g and C-g faults. Since the mean values are over the threshold when the problems first appear, these defects are simple to identify.

4.2. Multi-phase unsymmetrical faults

Furthermore, the detection method is verified for double line faults. There are 3 types of faults considered under multi-phase double line faults known as A-B, B-C, and A-C faults. These faults are simulated on given test system and the response of the method is presented in Figures 6, 7 and 8. In Figure 6, the current information and corresponding variation of means are presented for a A-B fault located at 15 km from relay point (middle of the line) with a phase-phase fault resistance of 10Ω, initiated at 1.42 sec. In case of B-C fault, fault location is 5 km, fault inception time 1.38 seconds, and fault resistance is 5Ω. In case of A-C, fault location is 25 km, fault inception time 1.53sec, and fault resistance is 1Ω.

Fig. 6. SNM-based method output during A-B Fault, a. currents, b. Means
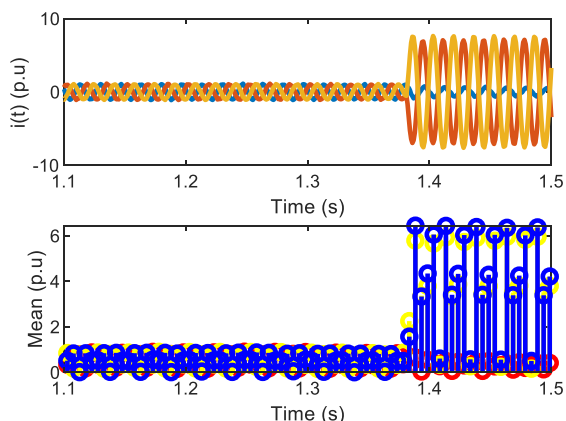
Fig. 7. SNM-based method output during B-C Fault, a. currents, b. Means
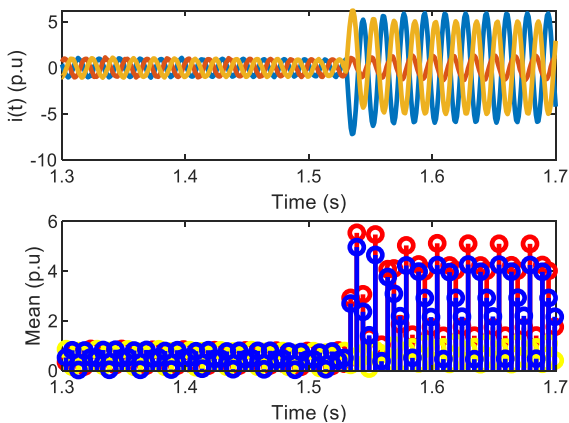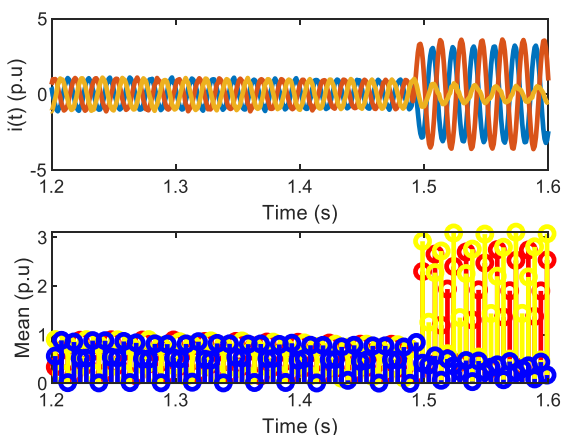
Fig. 8. SNM-based method output during A-C Fault, a. currents, b. Means

From the responses of the proposed method, it is clearly evident that the values of mean are exceeds thresholds after fault initiation and trip signals are generated as a result with 100% dependency. The phases involved in fault contact are recognised from the indices similarly to single line-to-ground faults, and the approach therefore also completes the task of faulty phase identification.

4.3. Line-to-line-ground faults

To investigate the performance of the proposed scheme during line-to-line-ground faults, 3 faults are simulated in the test system and the data is processed though the proposed SNM method to estimate the means of the currents in each window to check the performance of the algorithm. The 3 cases are A-B-g (Fig. 9), B-C-g (Fig. 10) and A-C-g (Fig. 11) faults.

The faults are simulated with the following parameters:
A-B-g: Fault location of 18 km, Fault resistance of 10Ω and inception time of 1.49 sec.
B-C-g: Fault location of 14 km, Fault resistance of 10Ω and inception time of 1.46 sec.
A-C-g: Fault location of 16 km, Fault resistance of 10Ω and inception time of 1.64 sec.
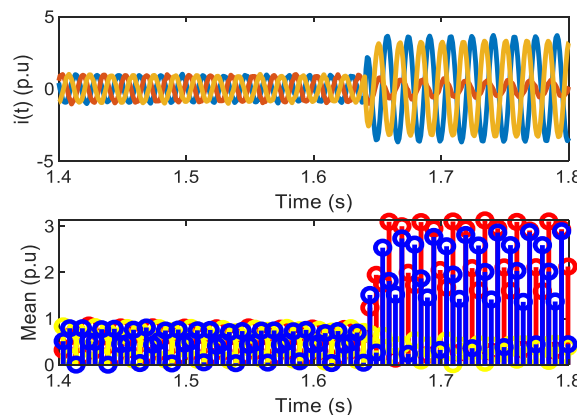

Fig. 9. SNM-based method output during A-B-g Fault, a. currents, b. Means

4.4 Three phase faults

The occurrence of symmetrical three phase faults is rare, but their detection is easy compared with single line-to-ground faults. The involvement of the three phases in fault produce higher detection indices in terms of magnitude compared to detection indices associated with single line and double line faults. To show the performance of the proposed method against three phase faults, an A-B-C fault is simulated with fault location of 28 km, fault inception time of 1.55 sec and fault resistance of 1Ω. Figure 12 shows the results of the SNM scheme. Even the fault location is remote end, the detection indices magnitudes are higher compered to L-g faults.
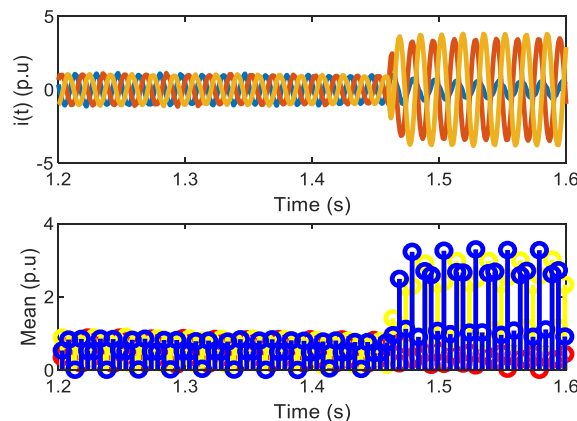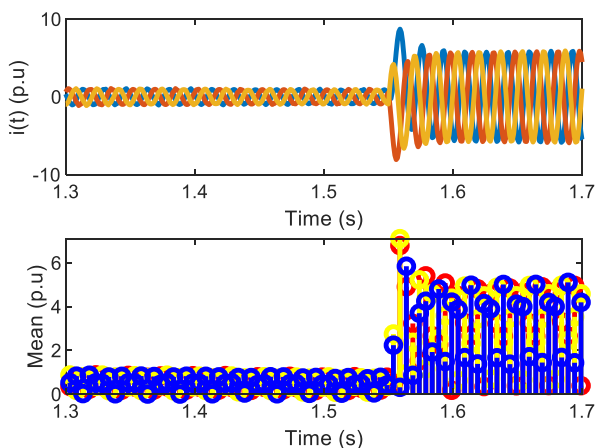

Fig. 10. SNM-based method output during B-C-g Fault, a. currents, b. Means

Fig. 11. SNM-based method output during A-C-g Fault, a. currents, b. Means

4.5 Three phase to ground faults

Three phase-to-ground faults are another typical fault with less probability occurrence. To check the validity of the proposed SNM scheme, an A-B-C-g fault is simulated with fault location of 8 km, inception time of 1.52 sec and fault resistance of 1Ω. The proposed method detects symmetrical faults quickly and provide correct faulty phase classification. The results associated with three phase symmetrical fault are presented in Figure 13.

Fig. 12. SNM-based method output during A-B-C Fault, a. currents, b. Means

Apart from the types of faults, fault parameters such as location, inception and resistance of faults are also influencing factors of protection attributes of such as dependability and speed. The effect of these factors are illustrated in the following sections to show the performance of the proposed scheme.
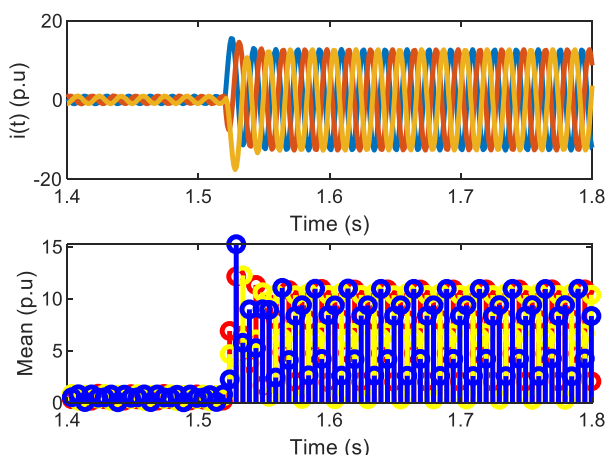

Fig. 13. SNM-based method output during A-B-C-g Fault, a. currents, b. Means

4.6 Effect of Fault location

The line impedance influence the magnitude of the current which further impacts the detection algorithm metrices since they are calculated from the variations of the voltage and current measured at receiving end. Fault location is the fault parameter changes line impedance and therefore detection indices. In this case, an A-g fault is considered to check the variation of the three phases SNM values by varying the location of the fault with inception time of 1.5 sec and fault resistance of the 5Ω. The line variation associated results are provided in Figure 14. Since the fault is in A-phase, the mean values corresponding to A-phase exceeds the pre-defined threshold and other mean values corresponding to B and C phases are still in normal range. Furthermore, the increase in the location value decreases the mean value since the

magnitude of the current decreases as impedance of the line increases with location. These observations are clearly visible in Figure 14. However, the proposed scheme is able to detect all the faults irrespective of the location of the fault shows the efficacy of the method.
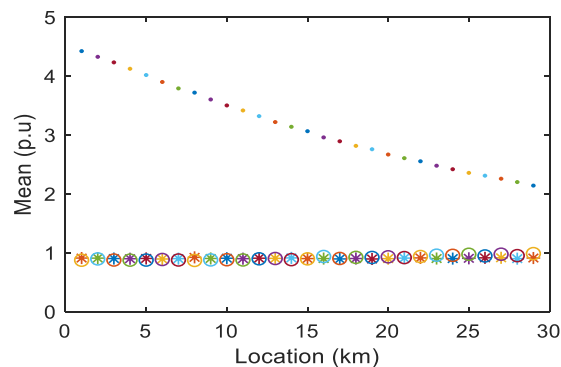
Fig. 14. SNM variation with fault location in case of L-g faults

4.7 Effect of fault inception angle

The fault inception time/angle is another fault parameter effect the detection algorithm index magnitude. Unlike fault location, the effect of the fault initiation time is minimum. However, the method is tested to verify the effect of the fault inception time since there are few algorithms are failed at zero inception angles. For this purpose, an A-B fault is considered with fault location of 15 km and fault resistance of 10Ω. The inception time of the fault is started at 1.4 sec and ended at 1.5 sec by considering 100 simulation cases in the 0.1 sec covers 100 inception times of the fault. The results are plotted in Figure 15. Since the fault is in A-B type, the mean values corresponding to A-and B-phases exceed the pre-defined threshold and other mean values corresponding to C phase are still in normal range. Furthermore, the variations in inception times changes the mean values. These observations are visible in Figure 15.
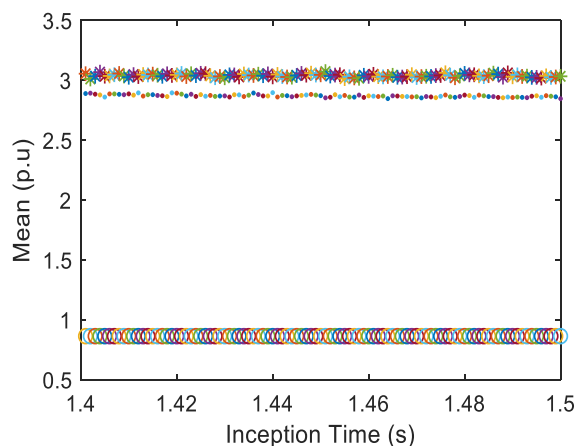
Fig. 15. SNM variation with fault inception in case of L-L faults

4.8. Effect of fault resistance

The fault resistance is the most influencing parameter among the location, inception and fault resistance. The effect of the variation of the fault resistance on signal means are plotted in Figure 16. To show these variations, B-g fault is simulated with fault location of 15km and fault initiation time of 1.5 sec. The fault resistance is varied from 1Ω to 20Ω, and indices of all phases are presented in Figure 16. Except the high resistive faults, all other faults are detected by the proposed scheme and faulty phase classification is also executed by the mechanism.
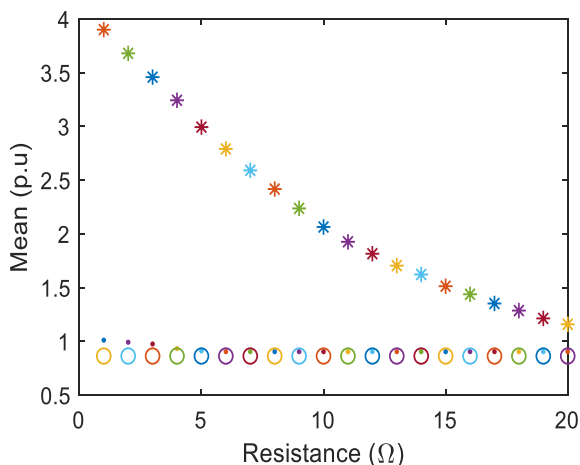

Fig. 16. SNM variation with fault resistance in case of L-g faults

4.9. Close in fault response

Apart from the regular fault cases, close in fault and simultaneous faults are simulated to check the performance of the proposed scheme under these special faults. Figure 17 shows the response of the proposed scheme when an A-g close in fault occurs at the grid bus. From the mean metrices, it is observed that the proposed SNM method is capable of detecting all typical faults along with normal faults.
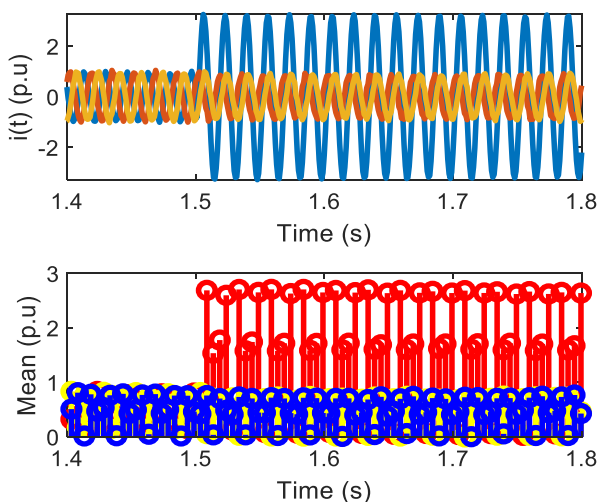

Fig. 17. SNM variation with fault resistance in case of L-g faults

Along with the acceptable detection results of the proposed method, faulty phase identification is another advantage of the method. Different types of faults are simulated to record the faulty phase information from the proposed method and results are reported in Table 1. In all cases, correct faulty phase is identified by the method. All these faults are detected within half cycle based on the mean variation of 2 windows reduces the fault detection time. The detection time information is also presented in the Table 1.

Table 1. Faulty phases and detection times of different faults using proposed method

Faulty phase classifications		
Fault type with parameters	Faulty phases	Detection time
A-g fault, 12 km, 1.4 sec, 10Ω	A	4 msec
B-g fault, 10 km, 1.4 sec, 20Ω	B	6 msec
C-g fault, 22 km, 1.4 sec, 30Ω	C	5 msec
A-B fault, 2 km, 1.4 sec, 1Ω	A,B	4 msec
B-C fault, 6 km, 1.4 sec, 5Ω	B,C	3 msec
A-C fault, 8 km, 1.4 sec, 4Ω	A,C	4 msec
A-B-g fault, 24 km, 1.4 sec, 10Ω	A,B	3 msec
B-C-g fault, 15 km, 1.4 sec, 10Ω	B,C	3 msec
A-C-g fault, 17 km, 1.4 sec, 10Ω	A,C	4 msec
A-B-C fault, 28 km, 1.4 sec, 5Ω	A,B,C	7 msec

5. Comparisons

Apart from the extensive simulation studies to show the performance of the proposed scheme at various types of the faults located at different distances with wide range of fault inception angles and fault resistances, it is necessary to check its performance at typical case studies. To validate the method at typical fault cases, a remote end fault is simulated. Additionally, the response of the method is compared with other standard methods. For simulation study, an A-g fault is considered with fault location of 28.8 km from the relay end, initiated at 1.5 sec with a fault resistance of 10Ω. For comparison, two methods are opted. In first method, mean-based estimation is used since the proposed method also used mean of the current samples. Wavelet transform method is used as second to show the merits of the proposed scheme. These methods are extensively used for fault detection studies

as discussed in section1 fails to provide correct trip during the simulated fault case. However, the proposed method is able to identify the fault located at remote terminal shows the effectiveness of the proposed method. All the cumulative results are presented in Figure 18.
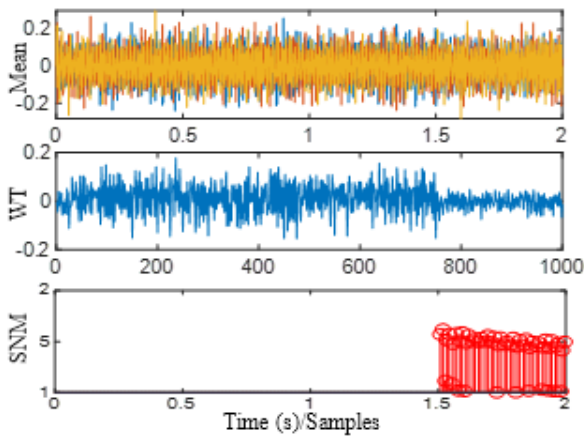
Fig. 18. Response of the proposed scheme during remote end fault

6. Conclusion

In this paper, SNM based new protection scheme is proposed to protect the distribution system connected with wind farm exports electrical power to main grid. The proposed scheme provide accurate decisions during faults in quick time. Along with the detection, faulty phases are identified by the proposed algorithm is an added advantage of the method. Along with normal faults, remote end faults are also detected by the method reliably and provided correct decisions to generate the trip commands. The method is dependable irrespective of the fault parameters and fault types. Due to symmetry concept incorporated in the mechanism, the method is applicable to any network. In future, the metrices are used to locate the faults with the help of artificial and machine leaning algorithms.

References

[1] A. M. Colak, and O. Kaplan, "A review on the efficiency increment in a power system using smart grid technologies", In 2021 9th International Conference on Smart Grid (icSmartGrid), IEEE, pp. 192-196, June 2021.

[2] A. Gonzalez, Daniel, E.M.G.Toro, M. Más-López, and S. Pindado, "Effect of distributed photovoltaic generation on short-circuit currents and fault detection in distribution networks: A practical case study", Applied Sciences, vol. 11, no. 1, pp.405-420, 2021.

[3] E. Zonkoly, and M. Amany, "Fault diagnosis in distribution networks with distributed generation", Electric Power Systems Research, vol.81, no. 7, pp.1482-1490, 2011.

[4] M.Y Nsaif, M.S. Hossain Lipu, A. Ayob, Y. Yusof, and A. Hussain, "Fault Detection and Protection Schemes for Distributed Generation Integrated to Distribution Network: Challenges and Suggestions", IEEE Access, vol. 9, pp.142693-142717, 2021.

[5] A.K.Pradhan, G.Joos,"Adaptive distance relay setting for lines connecting wind farms", IEEE Trans Energy Conv, vol. 22, pp.206–13, 2007.

[6] H.Sadeghi, "A novel method for adaptive distance protection of transmission line connected to wind farms", International Journal of Electrical Power & Energy Systems, vol.43, no.1, pp.1376-82, 2012.

[7] A.Hooshyar, M.A.Azzouz, E.F.El-Saadany, "Distance protection of lines connected to induction generator-based wind farms during balanced faults", IEEE Transactions on Sustainable Energy, vol.5, no.4, pp.1193-203, 2014.

[8] M.Jing, W.Zhang, J.Liu, J.S.Thorp, "A novel adaptive distance protection scheme for DFIG wind farm collector lines", International Journal of Electrical Power & Energy Systems, vol.94, pp.234-244, 2018.

[9] A. Ghorbani, H.Mehrjerdi, N.A.Al-Emadi, "Distance-differential protection of transmission lines connected to wind farms", International Journal of Electrical Power & Energy Systems, vol.89, pp.11-18, 2017.

[10] N. El Halabi, M. García-Gracia, J. Borroy, and J. L. Villa, "Current phase comparison pilot scheme for distributed generation networks protection", Applied Energy, vol. 88, no. 12, pp.4563-4569, 2011.

[11] K. Dubey, and P. Jena, "Impedance angle-based differential protection scheme for microgrid feeders", IEEE Systems Journal, vol. 15, no. 3, pp. 3291-3300, 2020.

[12] P.K. Ray, B. K. Panigrahi, P.K. Rout, A. Mohanty, and H. Dubey, "Fault detection in an IEEE 14-bus power system with DG penetration using wavelet transform", In Computer, Communication and Electrical Technology, pp. 221-225. CRC Press, 2017.

[13] H.R. Baghaee, D. Mlakić, S. Nikolovski, and T. Dragicević, "Support vector machine-based islanding and grid fault detection in active distribution networks", IEEE Journal of Emerging and Selected Topics in Power Electronics, vol. 8, no. 3, pp.2385-2403, 2019.

[14] M. Manohar, E. Koley, and S. Ghosh, "Microgrid protection under wind speed intermittency using extreme learning machine", Computers & Electrical Engineering, vol.72, pp.369-382, 2018.

[15] G. Ashika, S. R. Mohanty, and J.C. Mohanta, "Microgrid protection using Hilbert–Huang transform based-

differential scheme", IET Generation, Transmission & Distribution, vol.10, no. 15, pp. 3707-3716, 2016.

[16] B. Anudeep, and P.K. Nayak, "Transient energy based combined fault detector and faulted phase selector for distribution networks with distributed generators", International Transactions on Electrical Energy Systems, vol. 30, no. 4, pp. e12288, 2020.

[17] C.D. Prasad, M. Biswal, and A.Y. Almoataz, "Adaptive differential protection scheme for wind farm integrated power network", Electric Power Systems Research, vol. 187, pp. 106452, 2020.

[18] M. Kavi, Y. Mishra, and M. Vilathgamuwa, "Morphological fault detector for adaptive overcurrent protection in distribution networks with increasing photovoltaic penetration", IEEE Transactions on Sustainable Energy, vol. 9, no. 3, pp. 1021-1029, 2017.

[19] S. Roy, and S. Debnath, "PSD based high impedance fault detection and classification in distribution system", Measurement, vol. 169, pp. 108366, 2021.

[20] K. Anjaiah, P. K. Dash, and M. Sahani, "Detection of faults and DG islanding in PV-Wind DC ring bus microgrid by using optimized VMD based improved broad learning system", ISA Transactions, 2022.

[21] R.Kumar, C.D.Prasad, and M.Biswal, "Detection and Identification of Faulty Phase in a Thyristor Compensated Transmission Network Integrated with DFIG-Based Wind Farm", In Recent Advances in Power Systems, pp. 635-648. Springer, Singapore, 2022.

[22] C.D. Prasad, M. Biswal, and P. Ray, "Enhancing fault detection function in wind farm-integrated power network using Teaching Learning-Based Optimization technique", International Transactions on Electrical Energy Systems, vol.31, no.10, pp.e12735, 2021.

[23] A. Colak, and K. Ahmed, "A Brief Review on Capacity Sizing, Control and Energy Management in Hybrid Renewable Energy Systems", In 2021 10th International Conference on Renewable Energy Research and Application (ICRERA), pp. 453-458, September 2021

[24] O.V.G. Swathika,"LUT assisted adaptive overcurrent protection of reconfigurable microgrids", International Journal of Smart Grid-ijSmartGrid, vol.2, no. , pp.13-26, 2018.

[25] E.Bekiroglu, and M.D.Yazar, "Improving fault ride through capability of DFIG with fuzzy logic controlled crowbar protection", In 2022 11th International Conference on Renewable Energy Research and Application (ICRERA), pp. 374-378, 2022.

[26] A.K. Gangwar, and A.G.Shaik, "Wavelet Based Transmission Line Protection Scheme Using Centroid Difference and Support Vector Regression", In 2018 7th International Conference on Renewable Energy Research and Applications (ICRERA), pp. 1184-1189, 2018.